

Review

# A Recent Review of Primary Hydrogen Carriers, Hydrogen Production Methods, and Applications

Risheng Li <sup>1,2,\*</sup> and Hajime Kawanami <sup>1,2,\*</sup> 

<sup>1</sup> Master's/Doctoral Program in Chemistry Degree Programs in Pure and Applied Sciences, Graduate School of Science and Technology, University of Tsukuba, 1-1-1 Tennoudai, Tsukuba 305-8571, Ibaraki, Japan; li-risheng@aist.go.jp

<sup>2</sup> Interdisciplinary Research Center for Catalyst Chemistry, National Institute of Advanced Industrial Science and Technology, Central 5, 1-1-1 Higashi, Tsukuba 305-8565, Ibaraki, Japan

\* Correspondence: h-kawanami@aist.go.jp; Tel.: +81-70-4836-4801

**Abstract:** Hydrogen is a promising energy carrier, especially for transportation, owing to its unique physical and chemical properties. Moreover, the combustion of hydrogen gas generates only pure water; thus, its wide utilization can positively affect human society to achieve global net zero CO<sub>2</sub> emissions by 2050. This review summarizes the characteristics of the primary hydrogen carriers, such as water, methane, methanol, ammonia, and formic acid, and their corresponding hydrogen production methods. Additionally, state-of-the-art studies and hydrogen energy applications in recent years are also included in this review. In addition, in the conclusion section, we summarize the advantages and disadvantages of hydrogen carriers and hydrogen production techniques and suggest the challenging tasks for future research.

**Keywords:** hydrogen; carrier; production; water; methanol; methane; ammonia; formic acid



**Citation:** Li, R.; Kawanami, H. A Recent Review of Primary Hydrogen Carriers, Hydrogen Production Methods, and Applications. *Catalysts* **2023**, *13*, 562. <https://doi.org/10.3390/catal13030562>

Academic Editors: Concetta Ruocco and Marco Martino

Received: 30 January 2023

Revised: 2 March 2023

Accepted: 6 March 2023

Published: 10 March 2023



**Copyright:** © 2023 by the authors. Licensee MDPI, Basel, Switzerland. This article is an open access article distributed under the terms and conditions of the Creative Commons Attribution (CC BY) license (<https://creativecommons.org/licenses/by/4.0/>).

## 1. Introduction

Since 1800, coal, oil, and gas have accounted for major world's fossil fuel consumption. Since the Industrial Revolution, the use of these energy resources has dramatically increased and now plays a dominant role in the global energy consumption [1]. Although nonrenewable energy has been the basis of human societies' economic and technological development (84% of global primary energy in 2019 [2]), the unrestricted use of fossil fuels has resulted in several negative impacts. For instance, fossil fuels are being combusted to provide different forms of energy, consequently releasing tons of air pollutants, which are responsible for nearly one in every five deaths worldwide [3]. In addition, CO<sub>2</sub>, the most significant driver of global warming, is produced massively during combustion, which has led to a 0.85 °C annual average temperature anomaly in 2021 [4]. However, according to the IPCC special report on the impacts of global warming due to the increase in the temperature of 1.5 °C above pre-industrial levels, greenhouse gas emissions over the next decades should be lower, and net zero CO<sub>2</sub> emissions globally should be reached by 2050 [5].

To meet these goals, a rapid transition from fossil fuels to low-carbon energy sources is required. As a result, global energy industries have transformed their orientation toward developing technologies for low-carbon, green, and clean energy supplies. In this context, a growing number of researchers have focused on hydrogen gas as a potential clean energy source with 142,351 kJ/kg of combustion heat, which is 3, 3.9, and 4.5 times greater than that of gasoline, ethanol, and coke, respectively [6]. These advantages of hydrogen gas promote hydrogen energy as a feasible technology route for global energy transition and have become a hot topic in the world's energy sector in recent decades. To date, 18 countries representing 70% of the world's economy have already deployed strategic decisions for hydrogen energy solutions. In Hydrogen Insights 2021, the World Hydrogen Council

noted that the membership of the World Hydrogen Council has grown from 60 to over 100 since 2020. By early 2021, over 30 countries have announced hydrogen roadmaps and 228 large-scale hydrogen projects across the value chain, and governments worldwide have committed more than \$70 billion in public funding [7].

However, the wide application of hydrogen energy is limited in terms of the safety efficiency of storage and transportation owing to the unique physical properties (low and high energy density). With the development of new technologies, many hydrogen carriers have been developed to meet these requirements and push the utilization of this clean energy source.

In this review, we summarize the characteristics of primary hydrogen carriers and their relative production methods and assess state-of-the-art applications to systematically present the development status of hydrogen energy utilization. Moreover, this review also focuses on the advantages and disadvantages of hydrogen carriers and hydrogen production techniques, and suggests the challenging tasks for future research.

## 2. Hydrogen Carriers and Production Methods

### 2.1. Water ( $H_2O$ )

Water, which covers approximately 70.8% of the globe, is one of the most abundant compounds on the Earth. The total volume of water on the Earth is approximately 1386 million cubic kilometers, 96.5% of which is distributed in the oceans. Thus, water is a potential hydrogen carrier, abundant in nature. In addition, many water-based hydrogen production methods have been developed worldwide.

#### Water Electrolysis

Researchers have developed water electrolysis technologies for 200 years since Nicholson and Carlisle first discovered the process of decomposing water into hydrogen and oxygen by electrolysis [8]. In the early 21st century, less than 1% of global hydrogen production was achieved by applying these techniques because of the relatively high energy consumption, cost, and maintenance of current electrolyzers [9]. Until recently, electrolyzer manufacturing capacity reached approximately 8 GW per year; the completion of all projects under construction will result in 134–240 GW of installed electrolyzer capacity by 2030, double the expectations from 2021 [10,11].

Figure 1 shows a traditional simple electrochemical cell [11,12]. The central part of the electrolysis unit is an electrochemical cell filled with pure water as the electrolyte and two electrodes connected to an external power supply. When a specific voltage, called the critical voltage, is reached between the two electrodes, hydrogen is produced at the negatively polarized electrode (cathode), and oxygen is generated at the positively polarized electrode (anode). The amount of gas produced per unit time is related to the flow of current in an electrochemical cell.

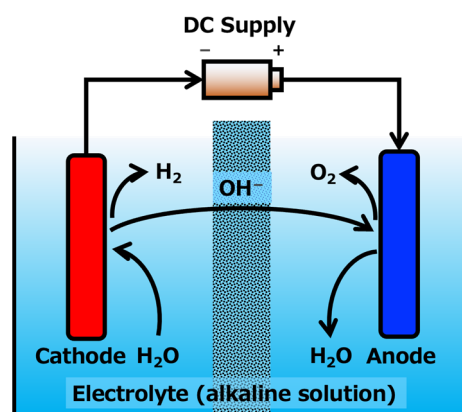


Figure 1. Scheme of a traditional simple electrochemical cell.

Three types of water electrolysis techniques can be employed based on the electrolyte used: (i) alkaline electrolysis (AEL), (ii) proton exchange membrane electrolysis (PEMEL), and (iii) high-temperature solid oxide electrolysis (HTEL) [13–16].

As for AEL (Figure 2), electrolyzers typically consist of an electrode, a microporous separator, and an alkaline aqueous electrolyte containing KOH or NaOH. Nickel with a catalytic coating is the most common cathode material used in alkaline electrolyzers, whereas nickel and copper metals coated with metal oxides are frequently used as anodes. The hydrogen evolution reaction (HER), oxygen evolution reaction (OER), and overall cell reactions conducted using AEL are shown in Equations (1)–(3).



AEL offers a relatively wider choice of electrocatalysts. However, the HER activity in an alkaline electrolyte is generally lower than that in an acidic electrolyte [16,17], limiting the performance of AEL. In addition, other major drawbacks of AEL that lower its beneficial properties are low partial load range, limited current density, and low operating pressure [17,18]. To improve this technique, in recent years, researchers have demonstrated that AEL at high temperatures leads to a dramatic reduction in cell voltages, which is promising for increasing current density and efficiency [18,19].

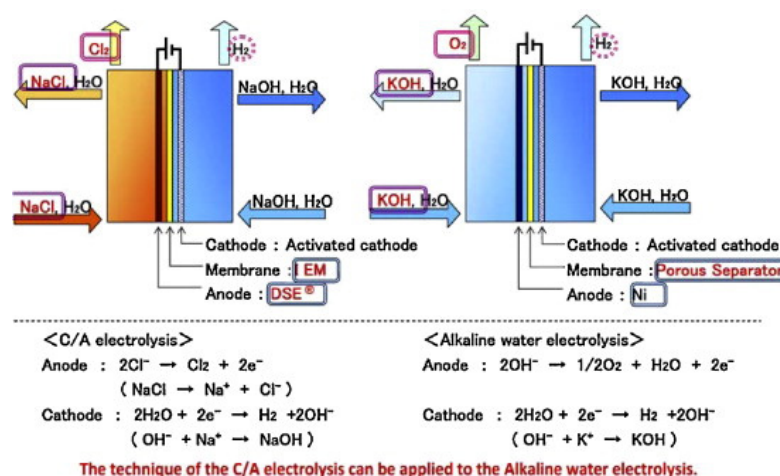


Figure 2. Schemes for AEL, alkaline electrolysis [20,21]. Reprinted with permission from [20].

PEMEL (shown in Figure 3) is a method based on applying a proton exchange membrane. The common practice is to use DuPont's Nafion membrane with high proton conductivity ( $0.1 \pm 0.02 \text{ Scm}^{-1}$ ). Ultrapure water is supplied to the anode to generate  $\text{O}_2$  gas, and hydrons are selectively passed through the membrane to reach the cathode, obtaining electrons to produce  $\text{H}_2$  gas. The half-cell reactions are shown in Equations (4) and (5).



PEMEL has the following benefits: (1) better safety and reliability because there is no corrosive electrolyte circulating in the cell package; (2) certain materials can withstand high differential pressure without damage and are effective in preventing gas mixing; (3) a thickness of a few millimeters per square centimeter and current of one ampere per square centimeter can be expected so that the cells can operate with a current of a few amperes per square centimeter [19,20]. Despite the advantages of using PEMEL, state-of-the-art

electrocatalysts composed of noble metals are applied to develop electrodes to achieve the higher activity, leading to a significant increase in the cost of PEMEL production [21].

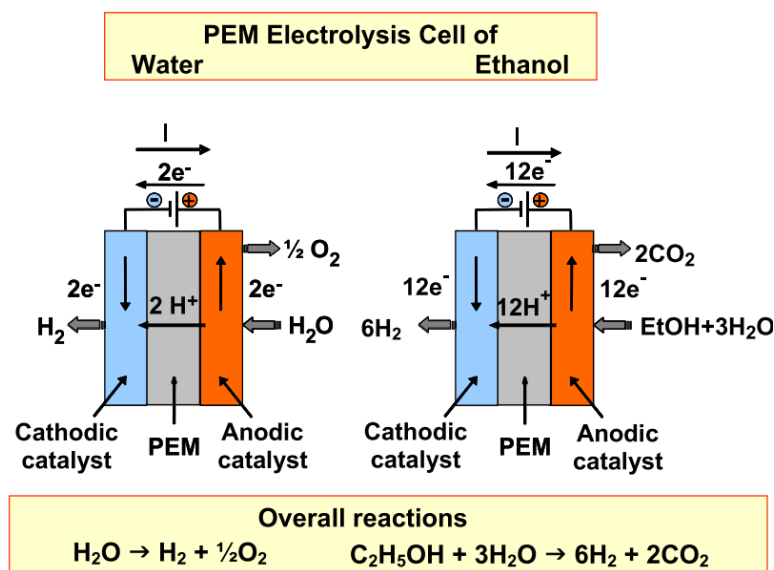


Figure 3. Scheme for PEMEL, proton exchange membrane electrolysis [22,23]. Reprinted with permission from [22].

In the 1980s, Donitz and Erdle first developed the HTEL (Figure 4). Although HTEL technology is characterized by extremely high operating temperature (500–850 °C) and high pressure, it attracted considerable attention due to its ability to produce ultrapure hydrogen with great efficiency [24,25]. The reactions occurring in a solid oxide electrolyzer cell are shown in Equations (6) and (7).

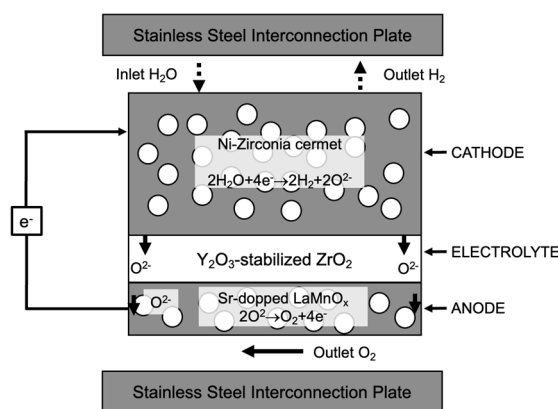
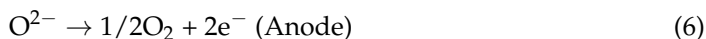


Figure 4. Scheme for HTEL, high-temperature solid oxide electrolysis. Reprinted with permission from [23].

In the past few years, ceramic proton-conducting materials have been studied and developed owing to their good efficiency and excellent ionic conductivity at high operating temperatures [12]. However, one of the barriers to the commercialization of HTEL is related to instability and degradation, such as chemical/electrochemical degradation, structural degradation, and mechanical failure caused by thermal stress [26–28]. To overcome these

drawbacks, researchers are exploring the mechanisms of electrode degradation [24,29] and electrolyte degradation [30]. Moreover, the surface modification of lanthanum strontium manganite, one of the oldest oxygen/air commercial electrode materials, was also explored. It has been demonstrated that the oldest material is highly effective in prolonging the durability of oxide electrolyzer cells.

Even though the use of these technologies for hydrogen production is evident, mass production is challenging, owing to technical restrictions in terms of efficiency, cost, and stability. However, applying electrocatalysts to water splitting is an efficient and economical method to produce environmentally friendly hydrogen. Generally, electrocatalysts can be divided into two types: noble-metal-based and non-noble-metal catalysts [31,32].

Noble-metal-based catalysts, such as iridium-based OER and Pt-based HER, are commonly used because of their high stability, low Tafel value, and small overpotential. However, their high price and rare reserves limit their commercial application [33,34]. Thus, producing highly active catalysts at low cost is urgently needed. Alloying noble metals with nonprecious metals can significantly reduce the cost of electrocatalysts while maintaining their high activities or even achieving better properties. Recently, Sun et al. reported the adoption of a multistep consequential-induced strategy to construct a core-shell  $Pt_x@Ni_y$  with high catalytic efficiency and stability, and the electrolytic overall water-splitting at  $10\text{ mA}\cdot\text{cm}^{-2}$  can be driven by a voltage of only 1.485 V by optimizing the feeding ratio of PtNi [35].

Alternatively, it is more efficient to lower the cost of electrocatalysts by substituting noble metals with non-noble metals. Transition metals, such as Ni, Co, Fe, and Mn, have been extensively explored as potential substitutes for noble metals in electrolytes for large-scale hydrogen production because of their high abundance, low cost, high corrosion resistance, and high activity in alkaline environments. Ni-based electrocatalysts, such as nickel oxides, nickel metal alloys, and N-doped nickel alloys, have largely been explored due to their promising performance. Recently, Tang et al. directly manufactured nickel-based electrocatalysts with glutenlike cubic structures using a photocuring 3D printing method, which showed a remarkably low overpotential of 34 mV at a current density of  $10\text{ mA}\cdot\text{cm}^{-2}$  with the incorporation of titanium [36].

## 2.2. Methane and Methanol

Methane ( $\text{CH}_4$ ) is a hydrocarbon that is the main component of natural gas. Currently, methane is obtained from natural gas, coal, and various chemical reactions. However, methane is also a potent greenhouse gas, which has more than 20 times the heat-trapping potential compared to carbon dioxide. Hence, the presence of methane significantly affects global temperature and climate systems.

Methanol ( $\text{CH}_3\text{OH}$ ), which consists of only one oxygen atom, one carbon atom, and four hydrogen atoms, is the simplest alcohol produced from natural gas and renewable resources. Using methanol as a hydrogen source has several advantages: (1) the energy consumption for methanol reforming is much lower compared to the reforming of natural gas, because the methanol reforming can be conducted at approximately  $300\text{ }^\circ\text{C}$ , which is a considerably lower temperature than that required for natural gas reforming [37,38]; (2) methanol is a sulfur-free molecule; hence, only trace amounts of CO may be present in the reformat gas during methanol reforming; (3) methanol is a relatively stable and light liquid that is easier to store under common environmental conditions.

Through years of dedicated investigation by researchers worldwide, it has been found that methane and methanol are effective hydrogen carriers to produce hydrogen by applying catalytic technologies. In this review, four conventional methods are summarized: steam methane reforming (SMR) and methanol reforming (partial oxidation of methanol and autothermal reforming).

### 2.2.1. Steam Methane Reforming (SMR)

SMR is a common method used in the industry to produce hydrogen. The process includes the following catalytic steps: S-removal, prereforming, reforming, high-and-low temperature water–gas-shift reactions, methanation, and NO<sub>x</sub> removal [39]. The key steps are shown as Equations (8) and (9). A typical SMR system with CO<sub>2</sub> removal options is shown in Figure 5 [40].

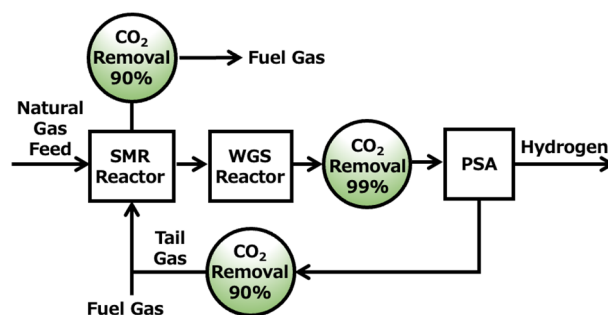


Figure 5. Scheme for a steam methane reforming (SMR) system with CO<sub>2</sub> removal options.

Although SMR can be chosen to conduct large-scale production in industries because of the reasonable price of natural gas, it is still challenging to miniaturize this process based on current technology [41]. In addition, SMR is commonly conducted at a high temperature, which needs to be maintained by supplying substantial energy [42]. Therefore, developing highly efficient catalysts with a long lifespan is important to lower the reaction temperature.

In this context, nickel-based catalysts have been developed and commercially applied for SMR because of their low cost and relatively high activity [43,44]; however, these Ni-based catalysts are easily deactivated at high temperatures owing to their decomposition [45,46]. To achieve better durability and stability, Song et al. successfully prepared a series of butyric acid-assisted nickel/alumina catalysts that showed stable performance for 1000 min with a 65% hydrogen yield [47]. Recently, Zhang et al. synthesized a PdNi bimetallic catalyst for light-driven hydrogen production, achieving a production rate of up to 260.9 mmol g<sup>-1</sup> h<sup>-1</sup> at 580 °C, and no noticeable activity drop of the catalyst was observed after five test cycles [48].

Additionally, the WGS reaction, which plays an important role in SMR to remove carbon monoxide from the syngas and produce hydrogen along with carbon dioxide, is sensitive to the reaction temperature, and the kinetic potential of the catalyst significantly influences the reaction rate of the target products. Opas Tojira et al. recently reported the evaluation of WGS over Ni/CeO<sub>2</sub> and Ni/CeSmO catalysts for H<sub>2</sub> production [49], also investigating the effects of the preparation method of catalysts and the influence of Sm loading on the catalytic activity [50]. According to the results of the catalytic activity measurements, the Ni/Ce5%SmO catalyst prepared by the combustion method showed the greatest performance. The authors correlated the enhanced activity of Ni/CeSmO with high surface area, and consequently the dispersion of metallic Ni and increase in surface acidity, which decreased the carbon deposition and accelerated CO absorption.

### 2.2.2. Methanol Reforming

The reactions involved in the methanol reforming process are shown in Equations (10)–(12). Figure 6 shows a schematic of the methanol reforming system.



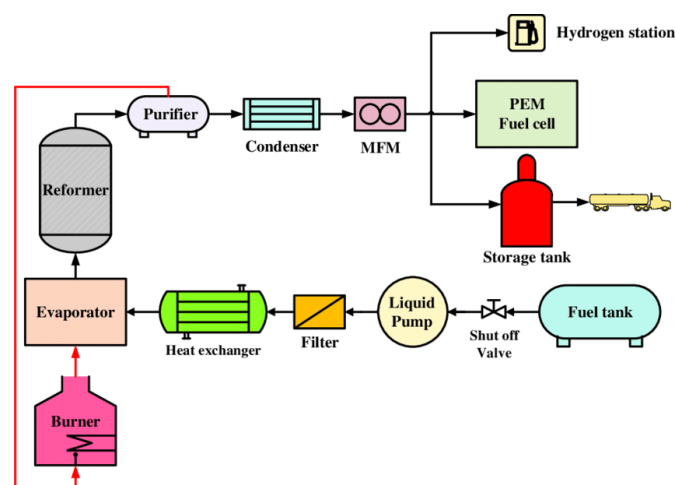


**Figure 6.** Scheme for a methanol reforming system. Reprinted with permission from [51].

An excellent methanol reforming catalyst must have remarkable catalytic activity and stability to ensure high methanol conversion with large hydrogen production. In addition, high selectivity should be considered, because it is necessary to inhibit the formation of CO during reforming, which could affect the yield and purity of hydrogen. Currently, two main categories of commercial catalysts are used for methanol reforming: copper-based catalysts and group 8–10 metal-based catalysts [52,53].

From the perspective of copper-based catalysts, CuO-ZnO-Al<sub>2</sub>O<sub>3</sub> catalysts, which are commonly utilized, exhibit relatively good performance [54,55]; however, copper-based catalysts have low stability at high temperatures. For instance, they suffer from spontaneous combustion, sintering, and deactivation [56]. To improve the stability of these catalysts, several studies have been conducted to explore novel preparation methods [57], the addition of promoters [58], and the development of enhanced catalytic systems [59–61]. Recently, Zheng et al. reported a nano-Cu<sub>2</sub>O/ZnO catalyst with double copper active sites, successfully producing hydrogen with 99% selectivity and a 36 h lifespan over 500 °C [62]. The nano-ZnO component plays a significant role, because it supports and scatters active sites to prevent the sintering and aggregation of copper active sites. Despite the high catalytic efficiency of the copper-based catalysts, there are still many drawbacks such as: (1) design and development of environmentally friendly protocol and (2) the microscopic insight into the reaction mechanism related to structure–activity relationships need further attention.

The metals of group 8–10 metal catalysts, such as Pd- and Ni-based catalysts, are characterized by better catalytic durability [63,64]. In 2022, Wang et al. suggested that a PdZn<sub>β</sub> alloy catalyst supported by ZnAl<sub>2</sub>O<sub>4</sub><sup>−</sup> could be synthesized even at low Pd loadings and reported 97% selectivity for CO<sub>2</sub> in the methanol steam reforming process [65]. Zhao et al. prepared a PdZn/ZnO/Al<sub>2</sub>O<sub>3</sub> catalyst, which showed better stability and excellent antioxidation ability in the methanol reforming process, coatings with different molar ratios by the coreduction method [66]. However, owing to the high cost of noble metals, researchers have been exploring inexpensive alternatives. Recently, Shen et al. also prepared a series of recyclable NiO/NaF catalysts of different Ni contents for the methanol reforming [67]. In this series, the 6%NiO/NaF provided the highest hydrogen production performance, achieving 94% methanol conversion, 100% H<sub>2</sub> selectivity, and 30 h stable operation at 450 °C. In addition, the catalytic activities of the recycled catalysts were comparable to those of fresh catalysts.

According to the trend in recent advancement, the catalytic aqueous phase reforming (APR) process has been applied to produce hydrogen from methanol (and other oxygenated

compounds). Generally, APR can be carried out under mild conditions (temperature: 220–270 °C; pressure: 30–60 bar) and this is one of the potential advantages of APR over the conventional steam reforming process, which takes place at around 800 °C [68]. Nowadays, monometallic catalysts (Pt, Ru, etc.) and bimetallic catalysts (Pt-Mo, Pt-Co, etc.) received considerable attention for their efficient catalytic performances. As for the guideline of the catalyst design, Giuseppe Pipitone et al. suggested two key points based on the mechanism to maximize the hydrogen production: (1) dehydrogenation, C–C bond breaking, H<sub>2</sub>O activation, and water gas shift reaction should be favored; (2) C–O bond breaking, methanation/Fischer–Tropsch, and dehydration should be avoided [69]. Moreover, the effect of support materials needs to be considered as one of the significant factors. Stekrova et al. explored the influence of different Ce, Zr, and La oxide supports for the APR of methanol and suggested that ZrO<sub>2</sub> and CeO<sub>2</sub> are useful supports for WGS because of their oxygen storage and mobility [70]. Concerning APR performance, the introduction of mixed oxides seems more beneficial for the improvement of the catalytic activity. Recently, Giulia Zoppi et al. reported that they successfully converted the waste carbon content (including methanol) in wastewater from a 15 kWh<sub>th</sub> Fischer–Tropsch plant to renewable hydrogen gas at mild temperature by using a Pt catalyst supported on activated carbon [71]. In terms of performance, the COD of the combination was reduced to 90% of its initial level, and the methanol conversion rate reached 100% after 4 h. Therefore, this work shows another potential pathway for the production of renewable energy from wastewater by using the APR process.

In the field of alternative energy storage and conversion devices, direct methanol fuel cell systems (DMFCs) have been considered one of the most important potential applications [72,73]. Recently, researchers have focused on the exploration of economical electrodes with high activity and durability for implementation in DMFC. As for the dual-functionalized electrocatalyst that is designed to maximize the performance of DMFCs, it can be divided into several types: monometallic catalysts (Pt-based [74], Pd-based [75], Au-based [76], etc.), bimetallic catalysts (Pt/Pd-based [77], Pt/Ni-based [78], Pt/Au based [79], Pt/Cu based [80], etc.), trimetallic catalysts (Pt/Ru/Co-based [81], Pt/Ir/Co-based [82], Pt/Au/Co-based [83], etc.), polymetallic and transition metal compounds-decorated catalysts, and nonprecious metal catalysts. Moreover, support materials perform a key role in the catalytic behavior, durability, and economic cost of the catalysts. Support materials that are effective for this purpose can be roughly classified into two categories: carbon-based/carbonaceous and noncarbonaceous. Generally, an ideal support material is required to have the following properties: (1) high electrical conductivity, (2) suitable porosity with mesopores, (3) high surface area, (4) excellent metal–support interaction, (5) electrochemical and thermal stability, and (6) good corrosion resistance [84]. Finally, from the perspective of DMFC, several challenging issues are required to be addressed: (1) relatively poor resisting ability of methanol crossover when the concentrated methanol (~9 M) is used in the fuel cell, (2) clear understanding of the reaction mechanisms, and (3) finding abundant alternatives to substitute expensive noble metals and developing “green” strategies that can extend from laboratory-scale to large scale.

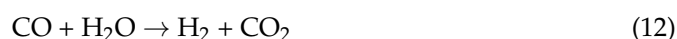


There is another alternative method known as partial oxidation of methanol (POM), which is widely applied for hydrogen production. In the POM process, methanol and oxygen are involved in the reaction, and the reactant mixture passes through a fixed catalyst bed reactor under atmospheric pressure. The overall reaction equation is described in Equation (10).

POM has the advantage of a quick start-up rate, and the overall reaction is an exothermic process with a rapid rate, thus a thermal control system is optional. However, the POM reaction is sensitive to the operating temperature, which means that a change in the operating temperature can shift the selectivity for the hydrogen production [85]. In addition, even without an external heat source, methanol can be fully oxidized to CO<sub>2</sub>

and H<sub>2</sub>O (as shown in Equation (10)) under certain conditions [86]. In addition to these drawbacks, POM involves complicated oxidation, steam reforming, and decomposition reactions [87]. Hence, POM produces relatively low-purity hydrogen because of its high CO content [88]; application to hydrogen fuel cells is restricted. To improve the efficiency of the POM for hydrogen production, Chen et al. prepared a novel Ni-Cu/Al<sub>2</sub>O<sub>3</sub> to promote the POM process, and 100% methanol conversion was achieved under all operating conditions and temperature ranging from 160 to 750 °C. Under the optimized operating conditions, the H<sub>2</sub> yield reached 2 mol (mol CH<sub>3</sub>OH)<sup>-1</sup>, which was better than that of the commercial h-BN-Pt/Al<sub>2</sub>O<sub>3</sub> catalyst [89].

Autothermal reforming (ATR) is another alternative method to methanol reforming for hydrogen production. ATR is a process involving partial oxidation and steam reforming reaction systems. ATR combines two chemical processes such as oxidation (Equation (11)) and reforming (Equation (12)). The fuel reacts with air and steam to produce a hydrogen-rich gas. The ATR of methanol uses enough heat generated by the exothermic POM to trigger a methanol stream reforming process. This replaces the external heat input to the reactor, making the system relatively simpler and less capital intensive. The natural gas feed reacts with oxygen in the combustion section, and this exothermic oxidation process supplies the heat necessary for the subsequent methanol reforming reaction. This process provides the advantages of an externally low energy requirement, low specific heat consumption, and relatively high gas-space velocity [90].



In terms of ATR reactor design, special packing of catalysts may be advantageous in methanol ATR. Richards et al. reported a catalytic stratified bed with a Cu-based catalyst [91]. This reactor showed remarkable conversion of methanol at low O<sub>2</sub>/MeOH ratios compared to the conventional packed-bed reactor configuration. Mu et al. successfully constructed a minireactor consisting of a reforming chamber, a catalytic combustion chamber, and two preheating chambers. This minireactor can operate an ATR of methanol at room temperature by producing hydrogen from the initial combustion of methanol. The optimum methanol conversion was 96.4%, and the converted gas contained 51.04% H<sub>2</sub> [92].

### 2.3. Ammonia

Ammonia (NH<sub>3</sub>) is a stable binary hydride and the simplest pnictogen hydride. Owing to its widespread application, global industrial production has reached 235 million tons since 2021. From the perspective of hydrogen production, ammonia is also considered an excellent inorganic hydrogen carrier owing to its inherent advantages, such as a remarkable hydrogen storage capability of 17.7 wt% at 20 °C. Moreover, it is easy to store and transport, because it exists in a liquid state under mild conditions. Furthermore, the mass production of ammonia from nitrogen can be performed by a primary method called the Haber–Bosch process [93].

#### Metal-Catalytic Reforming

Ammonia can produce hydrogen through a simple catalytic reforming reaction from 450 to 700 °C (Equation (13)) over supported metal catalysts and follows the order Ru > Ni > Rh > Co > Ir > Fe ≈ Pt > Cr > Pd > Cu ≈ Te, Se, and Pb supported on Al<sub>2</sub>O<sub>3</sub> [94].



However, the lack of catalysts with long-term stability limits the practical application of the catalytic reforming of ammonia for hydrogen production [95]. To address this issue, Jo et al. reported the successful synthesis of highly active Ru/La-Al<sub>2</sub>O<sub>3</sub> pellet catalysts, which sustained over 6700 h with the NH<sub>3</sub> conversion over 99.7% at 550 °C [96]. Additionally,

they packed a heat-transfer-enhanced NH<sub>3</sub> reformer with an advanced catalyst and applied a CO<sub>x</sub>-free heat source.

Contextually, Ru-based catalysts possess the highest activity for reforming NH<sub>3</sub>; however, the process is uneconomical because of the use of expensive Ru. Thus, several studies have been conducted to explore alternative catalysts. Recently, Xiao et al. prepared Ni/MgAl<sub>2</sub>O<sub>4</sub>-LDH, which is a nonprecious metal catalyst that shows 88.7% of NH<sub>3</sub> conversion and produces hydrogen at the rate of 1782.6 mmol g<sup>-1</sup> h<sup>-1</sup> at 600 °C, which remains stable over 30 h [97]. The authors reported that the excellent performance of the Ni/MgAl<sub>2</sub>O<sub>4</sub>-LDH catalyst originates from the high dispersity of Ni atoms on the MgAl<sub>2</sub>O<sub>4</sub>-LDH surface. Hayakawa et al. synthesized a series of zeolite (SA-600A)-based catalysts supported with RuCl<sub>3</sub>·nH<sub>2</sub>O and LiOH·H<sub>2</sub>O and optimized the ratio of the components. A catalyst with a mixing ratio of 40 g (SA-600A)/5 g RuCl<sub>3</sub>·nH<sub>2</sub>O/3 g LiOH·H<sub>2</sub>O showed the best activity, with a maximum NH<sub>3</sub> conversion of 99.87% at 490 °C [98].

To increase catalytic activity, selectivity, and prolong the lifespan of the catalysts, several transition metals, rare metals, alkali metals, and alkaline earth metals are commonly introduced as promoters. The mechanisms of the promotion by adding promoters have been summarized by Guo et al. [99]. The promoting effect of alkalis depends strongly on the chemical form used, of which alkali-NH has been shown to be an effective promoter [100]. Effective promoters are usually alkali or alkaline earth metals, which must be added as metal salts. These alkaline additives are more favorable for NH<sub>3</sub> decomposition than acidic precursors and electron-withdrawing groups. The available promoters are electron-donating groups that provide electrons to the antibonding state of the metal center to accelerate the nitrogen desorption rate-limiting step [101].

#### 2.4. Formic Acid

Formic acid (FA), the simplest carboxylic acid, is a colorless and low-toxicity liquid under ambient conditions that can be massively produced by the industry. In addition, FA exhibits strong hydrogen storage capability owing to its high gravimetric and volumetric H<sub>2</sub> capacities. Because of these beneficial properties, FA is considered a safe and economical hydrogen carrier for hydrogen storage and transportation.

##### 2.4.1. FA Catalytic Decomposition

There are two possible pathways of the FA dehydrogenation reaction (FADH): (1) through a decarboxylation process to afford CO<sub>2</sub> and H<sub>2</sub> (Equation (14)) and (2) through a decarbonylation process to afford CO and H<sub>2</sub>O (Equation (15)).



Notably, the selectivity may shift with changes in the reaction conditions, such as operating temperature and reactant concentration. In this context, optimizing the reaction conditions, especially catalyst screening, to find a suitable catalyst is vital to achieve the highest selectivity for the desired product. As for the category of FADH catalysts, they can be generally divided into two types: homogeneous and heterogeneous catalysts. The following sections summarize the features of the different types of FADH catalysts and the development of state-of-the-art catalysts.

##### 2.4.2. Homogeneous Catalysts for FADH

Compared with heterogeneous catalysts, homogeneous FADH catalysts are generally more active, highly selective, easily monitored spectroscopically, and feasible for modification.

The first homogeneous FADH catalyst, IrH<sub>2</sub>Cl (PPh<sub>3</sub>)<sub>3</sub>, was synthesized by Coffey in 1967, and it was reported that the highest TOF (1187 h<sup>-1</sup>) was achieved at an extremely high temperature of >1000 °C [102]. Decades later, the Puddetphatt group reported the

first study on the use of a locked binuclear catalyst,  $[\text{Ru}_2(\text{m-CO})(\text{CO})_4(\text{m-dppm})_2]$ , in the decomposition of FA and hydrogenation of  $\text{CO}_2$  [103,104]. In 2008, the excellent works on investigating various catalysts by Beller and Laurenczy received increased attention for developing an effective FADH process [105]. Laurenczy et al. applied an aqueous solution of  $[\text{Ru}(\text{H}_2\text{O})_6]^{2+}$  and commercially available  $\text{RuCl}_3$  with the water-soluble ligand meta-tri sulfonated triphenylphosphine for the decomposition of FA and achieved the highest conversion of 95% [106]. In 2013, Beller et al. reported an outperformed ruthenium catalyst,  $[\text{RuCl}_2(\text{C}_6\text{H}_6)]_2/\text{DPPE}$  (DPPE:1,2-Bis (diphenylphosphino)ethane), which allows continuous FA generation with over 1,000,000 TONs [107].

Furthermore, Fujita et al. reported the first reversible hydrogen storage system using a proton-switchable dinuclear  $\text{Cp}^*\text{Ir}$  catalyst that can be applied under mild conditions [108]. In 2013, Himeda et al. suggested a method for producing pressurized  $\text{D}_2$  or HD gas for laboratory use with FA and  $\text{D}_2\text{O}$  using Ir, Rh, and Ru complexes [109]. Recently, Albrecht et al. reported the development of a highly productive iridium FADH catalyst based on an iridium (III) center with a flexible pyridylidene-amine ligand containing chelating phenolate. This catalyst reached the highest TOF ( $280,000 \text{ h}^{-1}$ ) and TON of up to 3,000,000, which is the maximum compared to that reported for other catalysts [110]. Although a myriad of Ir-based catalysts has been developed, the mechanisms of the deactivation of the catalysts during the reaction are still unclear because of the lack of a suitable analytical method. In 2022, Li et al. reported that they developed a novel in situ UV-vis diffuse-reflectance spectroscopy system to monitor the FADH reaction catalyzed by the Ir-6DHBP complex [111]. They successfully obtained stable spectra corresponding to FA and Ir-6DHBP with high S/N ratio, which indicates that this new observation method could be promising to in situ investigate the decomposition process of the catalysts.

The more interesting property of formic acid dehydrogenation is the production of high-pressure gas without any compressing procedures. Laurenczy et al. reported the Ru complex can generate the gases ( $\text{H}_2$  and  $\text{CO}_2$ ) from formic acid by NMR analysis [112]. Kawanami et al. reported high-pressure gas generation using iridium (III) complexes and efficient separation from  $\text{H}_2/\text{CO}_2$  mixture under high-pressure conditions [113,114]. The prepared Ir complexes are possible to continuously produce high-pressure  $\text{CO}$ -free  $\text{H}_2$  in water upon the addition of concentrated FA (>99.5 wt%). In the same year, they investigated the solvent effects on high-pressure hydrogen gas production using Ru complexes having a dearomatized pyridine-based pincer  $\text{PN}^3\text{P}^*$  ligand and reported that 1,4 dioxane has the best performance to produce 20 MPa of hydrogen gas at  $80^\circ\text{C}$  [115]. In 2022, they indicated that the catalytic ability of the catalysts increased with the increasing electron-donating ability of the substituents [116].

Various noble metal catalysts have been investigated for FADH reactions, showing outstanding catalytic performance. However, to develop an economical process, non-noble metal catalysts have also been used as alternatives [117–119]. In 2010, Beller et al. reported the first light-driven Fe-based system for hydrogen generation from FA. In this system, using a catalyst synthesized in situ from inexpensive  $\text{Fe}_3(\text{CO})_{12}$  and additives, hydrogen evolution is possible under mild reaction conditions [120]. In 2019, Tanase et al. suggested the successful preparation of an asymmetric dinuclear copper-based catalyst,  $[\text{Cu}_2(\mu\text{-O}_2\text{CH})(\text{meso-L}^4)(\text{RNC})_2]^+$ , which exhibited relatively high catalytic activity for the FADH reaction [121]. Recently, Beller et al. reported an Mn-pincer homogeneous catalyst, which showed high catalytic activity (93% yield, TON = 2,000,000) in the presence of naturally occurring Lyn for the reversible hydrogenation of carbon dioxide to formic acid [122].

#### 2.4.3. Heterogeneous Catalysts for FADH

Heterogeneous catalysts have unique advantages over homogeneous FADH catalysts, such as easy catalyst/product separation and reusability. Thus, many researchers continue to develop advanced heterogeneous catalysts and attempt to apply them for practical  $\text{H}_2$  production [123,124]. Generally, heterogeneous catalysts can be divided into monometallic, bimetallic, and trimetallic catalysts.

Monometallic catalysts contain active nanoparticles of a single metal immobilized on the surfaces and centers of different structures. Recently, Basset et al. reported a promising heterogeneous approach toward FADH using a ruthenium  $\text{PN}^3\text{P}$  pincer complex,  $[\text{Ru}-\text{H}(\text{CO})(\text{i}^{\text{Bu}}\text{PN}^3\text{P})]$ , supported on KCC-1. This complex has an excellent TON of 600,000 without any detection of CO and shows exceptional stability (up to 45 cycles) [125]. In 2022, Guan et al. prepared a biomass-derived multifunctional  $\gamma\text{-Mo}_2\text{N}$  catalyst that exhibited excellent activity with the cooperation of K-containing, N-doped, and active sites [126].

Compared to that of monometallic catalysts, the catalytic activity of bimetallic catalysts is much more easily influenced by metal and metal supports. For example, Lu et al. reported the successful synthesis of a catalyst containing monodispersed Pd–Cr(OH)<sub>3</sub> nanoparticles loaded onto amine-functionalized mesoporous silica. This catalyst gave 100% hydrogen selectivity and conversion with an initial TOF of 3112 h<sup>−1</sup> at 100 °C, comparable to that of previously reported high-performance heterogeneous catalysts under similar reaction conditions [127]. In 2022, Lu et al. further anchored Pd–La(OH)<sub>3</sub> nanoparticles on an amine-functionalized porous carbon bowl (Pd–La(OH)<sub>3</sub>/N-PCB-NH<sub>2</sub>), and this catalyst showed a high TOF up to 9585 h<sup>−1</sup> at 100 °C [128].

In addition, a trimetallic catalyst was developed for the FADH reaction. Jiang et al. reported a CoAuPd nanoalloy supported on carbon that exhibits 100% H<sub>2</sub> selectivity and the ever highest values of TOF of 80 h<sup>−1</sup> without using any additives at room temperature [129]. More recently, Jiang et al. further reported the successful synthesis of an efficient catalyst, Au<sub>0.35</sub>Pd<sub>0.5</sub>Ir<sub>0.15</sub> nanoalloy supported on NH<sub>2</sub>-N-rGO, applied for FADH. DFT calculations revealed that introducing Ir to the AuPd alloys changed the initial adsorption conformation of HCOOH<sup>†</sup> and lowered the energy barrier for the rate-determining step of the FADH reaction. Thus, Au<sub>0.35</sub>Pd<sub>0.5</sub>Ir<sub>0.15</sub>/NH<sub>2</sub>-N-rGO displayed 100% H<sub>2</sub> selectivity, 100% FA conversion, and an initial TOF of up to 12,781.2 h<sup>−1</sup> without any additives [130].

### 2.5. Biomass

Compared with the majority of hydrogen production methods, the hydrogen production from biomass by applying biohydrogen technology is sustainable and environmentally friendly. Hydrogen-containing compounds can be used as feedstocks for hydrogen production, such as alcohol, hydrocarbons, biofuels, water, biomass, glycerol, etc. [131–134]. These other feedstocks can be efficiently produced from biomass (Figure 7).

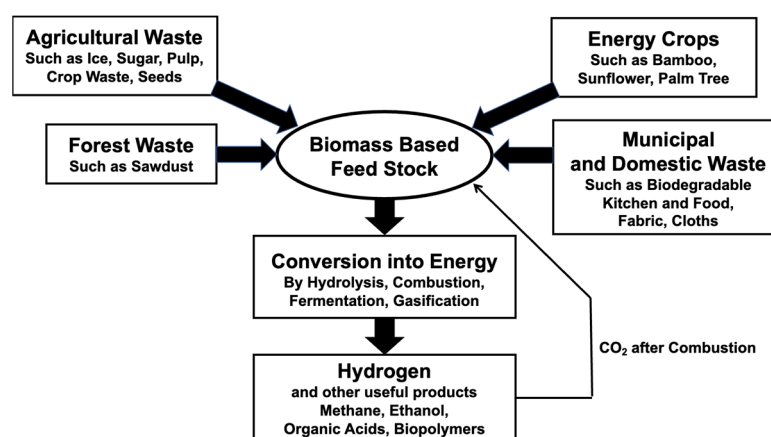


**Figure 7.** Various biomass sources and their conversion into H<sub>2</sub> and other useful products. Reprinted with permission from [135].

The biological hydrogen production methods can be divided into three categories: (1) fermentation, (2) pyrolysis, and (3) gasification. As for biomass fermentation, there are two types of methods: photofermentation and dark fermentation. Dark fermentation in bioreactors is easier and cheaper than photofermentation, because this method does not require solar input [136]. In addition, H<sub>2</sub> generation by dark fermentation has the capability

to generate H<sub>2</sub> from organic waste and thus to manage and stabilize biological waste prone to pollute the environment. Recently, Zhao et al. studied the use of corn stalk biochar remaining after anaerobic BioH<sub>2</sub> generation to increase BioH<sub>2</sub> production from corn stalk hydrolysates by fermentation [137]. The biochar resulted in a maximum BioH<sub>2</sub> production of 154.3 mL/H<sub>2</sub>/corn stalk.

As for the pyrolysis, the reaction yields coke, methanol, and other gases. In the high-temperature gasification process, the biological material is mainly converted into gas. The H<sub>2</sub>-rich gas is condensed in the pyrolysis oil, and H<sub>2</sub> can then be produced by steam reforming. This method gives a yield of  $12 \pm 17\%$  H<sub>2</sub> by dry basis mass [138]. To sustainably produce H<sub>2</sub> energy from the organic waste used as raw material, it must be fully renewable. Pokorna et al. reported the production of pyrolysis oil from three types of fecal sludge. Flash pyrolysis was performed at 500 °C with a maximum oil yield of 43.1% and moderate moisture present in the bio-oil obtained from a small amount of sludge [139]. Valle et al. studied the conversion of crude bio-oil to hydrogen-rich gas using Ni/La<sub>2</sub>O<sub>3</sub>-Al<sub>2</sub>O<sub>3</sub> catalysts. In a two-step system, SR of crude bio-oil produced a hydrogen-rich gas (93% H<sub>2</sub> is produced) [140].

As for gasification, it commonly uses biomaterials and coal, and is widely applied in many industrial methods. It deviates from pyrolysis and is therefore based on the fractional oxidation of the material composed of H<sub>2</sub>, CH<sub>4</sub>, CO<sub>2</sub>, CO, and N<sub>2</sub> identified as producer gases [141]. Florin et al. suggested that biomass steam gasification with CO<sub>2</sub> capture using CaO sorbents as a possible method for renewable and sustainable H<sub>2</sub> production [142]. In the absence of CO<sub>2</sub> capture material, most experimental results of biomass steam gasification exhibited H<sub>2</sub> concentrations in the range 40–50% (*v/v*).

### 3. Applications of Hydrogen Energy

Hydrogen is considered the most promising clean energy source of the 21st century because of its diverse sources, high calorific value, good thermal conductivity, and high reaction rate. Thus, many researchers have contributed towards developing hydrogen energy systems to realize hydrogen gas utilization. In this section, several practical applications of hydrogen energy are summarized.

#### 3.1. Hydrogen Fuel Cell (HFC)

Hydrogen fuel cells combine hydrogen and oxygen and produce only pure water as exhaust. Converting the chemical energy stored in H<sub>2</sub> gas into electrical energy can be used to drive electric motors or temporarily store energy, among other applications.

Fuel cell vehicles (FCVs) are among the most important applications of HFCs. The fuel cell generates electricity through a chemical reaction between hydrogen and oxygen in the air, and electricity is used to power the motor to drive the car. Fuel cells release only water instead of carbon dioxide (CO<sub>2</sub>) or other air pollutants; they are environmentally benign and show more than twice the energy efficiency of gasoline-powered cars. Hence, FCVs are expected to become the ultimate ecocars. In Japan, FCV sales began ahead of the world: Toyota Motor Corporation launched MIRAI in 2014, and Honda Motor Corporation launched Clarity Fuel Cell in 2016 [143]. The distance that an FCV can travel with a single hydrogen refill is approximately 650–750 km, and the hydrogen refill time is approximately 3 min, which is equivalent to that of a gasoline-powered vehicle.

In addition to commercial vehicles, Youon, a technology company in China, developed public electric bicycles powered by HFC, which can be used with the support of a smart public transportation system. This type of bicycle can be ridden for 70 km after one charge, with the highest speed of 23 km/h. Furthermore, to solve the problem of hydrogen storage safety, a low-pressure hydrogen storage device was developed, and a standardized scale production was formed, which reduced the hydrogen storage pressure from the original 30 to 2 MPa and increased the capacity of the hydrogen storage device by 40% [144].

### 3.2. As a Fuel in an Internal Combustion Engine (Hydrogen Internal Combustion Engine, HICE)

Hydrogen gas produces only pure water through the exhaust. Still, hydrogen as fuel in an internal combustion engine (ICE) generates NO<sub>x</sub> by reaction with nitrogen in air. Hence, for NO<sub>x</sub> combustion, a three-way catalyst and NO<sub>x</sub> catalyst are essential for combustion instead of superlean combustion. In addition, with the advent of fuel cells, which produce electricity by reacting hydrogen and oxygen, the value of hydrogen-fueled ICEs was misunderstood at the time. Recently, as the issue of carbon neutrality has become more serious, attention has been given to the production of hydrogen from surplus renewable energy, and the development of ICEs has been revived. However, mass production of fuel cells is expensive with the use of precious metals as catalysts, less durability than that of ICE, and capital investment for fuel cell stacks.

In contrast, ICEs can be cheaper, because various technologies of gasoline engines, such as direct injection, turbocharging, prechamber ignition, Miller cycle, lean combustion, and cylinder deactivation, can be applied for development. In addition, if the ICE can also be used in hybrid energy systems and plug-in hybrid systems combined with battery electric vehicles, it must be able to compete with fuel cells in terms of thermal efficiency [145].

In the early stage, Mazda and BMW developed an ICE, and BMW produced the first mass-produced vehicle with a 12-cylinder engine equipped with two separate fuel systems: hydrogen and petrol (bifuel system). For another example, Matsuda developed an ICE using Wankel rotary engines [146]. Recently, Toyota Motor Corporation (TMC) presented a racing vehicle with a 1.6 L ICE powered by hydrogen, and the Yamaha Group and TMC reported a prototype 5 L ICE with 450 horsepower in 2022.

### 3.3. As a Clean Fuel for the Steel Industry

Currently, the steel industry generally uses BF, NG, and COG gases as fuels. However, if large quantities of hydrogen or highly hydrogen-rich gases can be obtained at low prices, increasing the hydrogen content of the existing fuel system would improve the production efficiency because of the higher energy efficiency and heat value while reducing CO<sub>2</sub> emissions. The promising utilization of hydrogen or hydrogen-rich gas as fuels is mainly related to pellet production, sinter production, heating ladles, and reheating furnaces [147].

### 3.4. Energy Storage System

Given the high storage capacity of hydrogen, hydrogen-based energy storage systems have gained momentum in recent years. They can meet energy storage needs in a wide range, from short-term grid frequency regulation to medium- and long-term energy supply and demand balancing.

Numerous hydrogen storage projects have been launched worldwide, demonstrating the potential for widespread industrial use. DATAZERO is a project that was operated from 2015 to 2019 and aimed to investigate new ways to power and manage one cloud data center using on-site renewable energy sources and storage elements (such as photovoltaics, wind turbines, and fuel cells). More recently, the second stage of this project, called DATAZERO2, was conducted to improve the operation and design of cooperating data centers operated only with renewable energy sources [148].

Underground Sun Storage is a project developed to store seasonal and large-scale renewable energy in underground gas reservoirs. Until 2025, this project aimed to conduct interdisciplinary scientific and technical research on the energy future [149].

## 4. Conclusions and Perspectives

Hydrogen is a promising clean energy source because of its high energy density, high heat value, and environmental friendliness. To efficiently use hydrogen as an energy source, researchers have explored a myriad of hydrogen carriers and hydrogen production technologies.

Water, as an inorganic hydrogen carrier with high hydrogen content, is a nontoxic compound, which is abundant on the Earth. However, electrolysis of water followed by

the production of hydrogen still faces numerous challenges that could be the focus of the future research to implement this technology. For instance, the maximum current density is commonly required to be less than 0.45 mA/cm<sup>2</sup>. Additionally, the cost of an AEL system could be estimated at 900–1700 EUR/kW, which is far more expensive than the target cost predicted for 2025. Compared with other water electrolysis technologies, the PEMEL system has high load flexibility and capability to provide grid-balancing services, although it usually suffers mass transfer losses and a decrease in current density because of the blocking of the electrode pores. As for the HTEL system, besides the reduction in electrical energy consumption, another advantage is that efficiencies can reach 100% at current densities of industrial interest. However, some common issues of the HTEL system require attention such as quite long turn-on and turn-off steps, and a rather short lifespan because of the high temperature interdiffusion of the cell stacks and poisoning by the construction materials.

As discussed, ammonia, with its high hydrogen content up to 17.7%, has been considered a promising hydrogen carrier since 2000s because of its high energy density, ease of production, and long-term storage. However, the kinetics of ammonia decomposition is slow, limiting its wide industrial application. Regarding the LOHCs, including FA, methane, methanol, etc., they possess excellent properties that are close to crude oil. These characteristics correspond well with existing energy infrastructure, but investigations on their toxicity information and technical availability have only begun. Furthermore, bio-hydrogen technology that can deliver hydrogen from the transformation of biomass has recently become an important research topic. Although this technique is featured as a sustainable and environmentally friendly hydrogen production process, it needs significant future research to improve its H<sub>2</sub> generation rate and final yield.

Therefore, many corporations and organizations have contributed to the development of hydrogen technology and attempted to expand its application in various industries, including automobile, transportation, steel, and energy-storage systems. Their persistent efforts have established the way for human society to build an advanced hydrogen economy in the future.

**Author Contributions:** Conceptualization, R.L. and H.K.; writing—original draft preparation, R.L. and H.K.; writing—review and editing, H.K.; visualization, H.K.; supervision, H.K.; project administration, H.K.; funding acquisition R.L. and H.K. All authors have read and agreed to the published version of the manuscript.

**Funding:** This research was financially supported by the CANON Foundation, the New Energy and Industrial Technology Development Organization (NEDO), and the Japan Science and Technology Agency (JST), for the establishment of university fellowships toward the creation of science technology innovation (grant number JPMJFS2106).

**Data Availability Statement:** Not applicable.

**Acknowledgments:** R.L. and H.K. thank Maya Chatterjee for checking, improving, and correcting our manuscript.

**Conflicts of Interest:** The authors declare no conflict of interest.

## References

1. Ashton, T.S. *The Industrial Revolution 1760–1830*; OUP Catalogue, Oxford University Press: Oxford, UK, 1997.
2. Ritchie, H.; Roser, M.; Rosado, P. *Energy*; Our World Data: Oxford, UK, 2022.
3. Vohra, K.; Vodonos, A.; Schwartz, J.; Marais, E.A.; Sulprizio, M.P.; Mickley, L.J. Global mortality from outdoor fine particle pollution generated by fossil fuel combustion: Results from GEOS-Chem. *Environ. Res.* **2021**, *195*, 110754. [CrossRef]
4. NASA Global Climate Change. Global Surface Temperature | NASA Global Climate Change. Available online: <https://climate.nasa.gov/vital-signs/global-temperature/> (accessed on 17 February 2023).
5. IPCC. *Global Warming of 1.5 °C: IPCC Special Report on Impacts of Global Warming of 1.5 °C above Pre-Industrial Levels in Context of Strengthening Response to Climate Change, Sustainable Development, and Efforts to Eradicate Poverty*, 1st ed.; Cambridge University Press: Cambridge, UK, 2022.

6. Safari, F.; Dincer, I. A review and comparative evaluation of thermochemical water splitting cycles for hydrogen production. *Energy Convers. Manag.* **2020**, *205*, 112182. [CrossRef]
7. Hydrogen Council. Hydrogen Insights 2021. In *Hydrogen Council*; Hydrogen Council: Belgium, 2021.
8. Zoulias, E.; Varkaraki, E.; Lymberopoulos, N.; Christodoulou, C.N.; Karagiorgis, G.N. A Review on Water Electrolysis. *Tcjtst* **2004**, *4*, 41–71.
9. Santos, D.M.F.; Sequeira, C.A.C.; Figueiredo, J.L. Hydrogen production by alkaline water electrolysis. *Quím. Nova* **2013**, *36*, 1176–1193. [CrossRef]
10. IEA. Hydrogen. Available online: <https://www.iea.org/reports/hydrogen> (accessed on 30 December 2022).
11. Rashid, M.; Al Mesfer, M.; Naseem, H.; Danish, M. Hydrogen Production by Water Electrolysis: A Review of Alkaline Water Electrolysis, PEM Water Electrolysis and High Temperature Water Electrolysis. *Int. J. Eng. Adv. Technol.* **2015**, *4*, 2249–8958.
12. Sapountzi, F.M.; Gracia, J.M.; Weststrate, C.J.; Fredriksson, H.O.A.; Niemantsverdriet, J.W. Electrocatalysts for the generation of hydrogen, oxygen and synthesis gas. *Prog. Energy Combust. Sci.* **2017**, *58*, 1–35. [CrossRef]
13. Hu, X.; Liu, M.; Huang, Y.; Liu, L.; Li, N. Sulfonate-functionalized polybenzimidazole as ion-solvating membrane toward high-performance alkaline water electrolysis. *J. Membr. Sci.* **2022**, *663*, 121005. [CrossRef]
14. Wu, L.; An, L.; Jiao, D.; Xu, Y.; Zhang, G.; Jiao, K. Enhanced oxygen discharge with structured mesh channel in proton exchange membrane electrolysis cell. *Appl. Energy* **2022**, *323*, 119651. [CrossRef]
15. Sun, Y.; Hu, X.; Gao, J.; Han, Y.; Sun, A.; Zheng, N.; Shuai, W.; Xiao, G.; Guo, M.; Ni, M. Solid oxide electrolysis cell under real fluctuating power supply with a focus on thermal stress analysis. *Energy* **2022**, *261*, 125096. [CrossRef]
16. Strmcnik, D.; Uchimura, M.; Wang, C.; Subbaraman, R.; Danilovic, N.; Van Der Vliet, D.; Paulikas, A.P.; Stamenkovic, V.R.; Markovic, N.M. Improving the hydrogen oxidation reaction rate by promotion of hydroxyl adsorption. *Nat. Chem.* **2013**, *5*, 300–306. [CrossRef]
17. Carmo, M.; Fritz, D.L.; Mergel, J.; Stolten, D. A comprehensive review on PEM water electrolysis. *Int. J. Hydrog. Energy* **2013**, *38*, 4901–4934. [CrossRef]
18. Phillips, R.; Gannon, W.; Dunnill, C. *Alkaline Electrolysers*; Royal Society of Chemistry: London, UK, 2019; Chapter 2; pp. 28–58. [CrossRef]
19. Millet, P.; Andolfatto, F.; Durand, R. Design and performance of a solid polymer electrolyte water electrolyzer. *Int. J. Hydrog. Energy* **1996**, *21*, 87–93. [CrossRef]
20. Manabe, A.; Hashimoto, T.; Kashiwase, M.; Kurosaki, M.; Hayashida, T.; Hirao, K.; Shimomura, I.; Nagashima, I. Basic Study of Alkaline Water Electrolysis. *Electrochim. Acta* **2013**, *100*, 249–256. [CrossRef]
21. Xu, W.; Scott, K. The effects of ionomer content on PEM water electrolyser membrane electrode assembly performance. *Int. J. Hydrog. Energy* **2010**, *35*, 12029–12037. [CrossRef]
22. Coutanceau, C.; Jaubert, T.; Baranton, S.; Lamy, C. Clean Hydrogen Generation through the Electrocatalytic Oxidation of ethanol in a Proton Exchange Membrane Electrolysis Cell (PEMEC): Effect of the nature and structure of the catalytic anode. *J. Power Sources* **2014**, *245*, 927. [CrossRef]
23. Gómez, S.; Hotza, D. *Solid Oxide Electrolysers*; Keith Scott: Newcastle, UK, 2019; Chapter 5; pp. 136–179. [CrossRef]
24. Zhang, X.; Song, Y.; Wang, G.; Bao, X. Co-electrolysis of CO<sub>2</sub> and H<sub>2</sub>O in high-temperature solid oxide electrolysis cells: Recent advance in cathodes. *J. Energy Chem.* **2017**, *26*, 839–853. [CrossRef]
25. Laguna-Bercero, M.A. Recent advances in high temperature electrolysis using solid oxide fuel cells: A review. *J. Power Sources* **2012**, *203*, 4–16. [CrossRef]
26. Rashkeev, S.N.; Glazoff, M.V. Atomic-scale mechanisms of oxygen electrode delamination in solid oxide electrolyzer cells. *Int. J. Hydrog. Energy* **2012**, *37*, 1280–1291. [CrossRef]
27. Tietz, F.; Sebold, D.; Brisse, A.; Schefold, J. Degradation phenomena in a solid oxide electrolysis cell after 9000 h of operation. *J. Power Sources* **2013**, *223*, 129–135. [CrossRef]
28. Ebbesen, S.; Høgh, J.; Agersted, K.; Nielsen, J.; Mogensen, M. Durable SOC stacks for production of hydrogen and synthesis gas by high temperature electrolysis. *Fuel Energy Abstr.* **2011**, *36*, 7363–7373. [CrossRef]
29. Liu, Y.L.; Jiao, C. Microstructure degradation of an anode/electrolyte interface in SOFC studied by transmission electron microscopy. *Solid State Ion.* **2005**, *176*, 435–442. [CrossRef]
30. Knibbe, R.; Hauch, A.; Hjelm, J.; Ebbesen, S.; Mogensen, M. Durability of Solid Oxide Cells. *Green* **2011**, *1*, 141. [CrossRef]
31. Makarova, M.; Jirkovský, J.; Klementova, M.; Jirka, I.; Macounová, K.; Krtil, P. The Electrocatalytic Behavior of Ru<sub>0.8</sub>Co<sub>0.2</sub>O<sub>2-x</sub>—The Effect of Particle Shape and Surface Composition. *Electrochim. Acta* **2008**, *53*, 2656–2664. [CrossRef]
32. Lewis, N.; Nocera, D. Powering the Planet: Chemical Challenges in Solar Energy Utilization. *Proc. Natl. Acad. Sci. USA* **2006**, *103*, 15729–15735. [CrossRef]
33. Panwar, N.L.; Kaushik, S.C.; Kothari, S. Role of renewable energy sources in environmental protection: A review. *Renew. Sustain. Energy Rev.* **2011**, *15*, 1513–1524. [CrossRef]
34. Peng, L.; Ling, Z.; Shen, J.; Wei, Z. Self-Assembly- and Preshaping-Assisted Synthesis of Ultrathin Nitrogen-Doped Graphitic Carbon Lamellas Supported Molybdenum Carbide for Hydrogen Evolution Reaction. In *Electrochemical Society Meeting Abstracts*; The Electrochemical Society, Inc.: Pennington, NJ, USA, 2017; Volume MA2017-02, p. 2219. [CrossRef]

35. Xu, W.; Chang, J.; Cheng, Y.; Liu, H.; Li, J.; Yongjian, A.; Hu, Z.; Zhang, X.; Wang, Y.; Liang, Q.o.Q.-l.; et al. A multi-step induced strategy to fabricate core-shell Pt-Ni alloy as symmetric electrocatalysts for overall water splitting. *Nano Res.* **2021**, *15*, 965–971. [[CrossRef](#)]
36. Liyanage, D.R.; Li, D.; Cheek, Q.B.; Baydoun, H.; Brock, S.L. Synthesis and oxygen evolution reaction (OER) catalytic performance of Ni<sub>2-x</sub>Ru<sub>x</sub>P nanocrystals: Enhancing activity by dilution of the noble metal. *J. Mater. Chem. A* **2017**, *5*, 17609–17618. [[CrossRef](#)]
37. Zhang, J.; Zy, T.; Peng, C. Direct Photo-curing 3D Printing of Nickel-based Electrocatalysts for Highly-efficient Hydrogen Evolution. *Nano Energy* **2022**, *102*, 107615. [[CrossRef](#)]
38. Izquierdo, U.; Barrio, V.L.; Cambra, J.; Requies, J.; Güemez, M.B.; Arias, P.L.; Kolb, G.; Zapf, R.; Gutiérrez, A.M.; Arraibi, J.R. Hydrogen production from methane and natural gas steam reforming in conventional and microreactor reaction systems. *Int. J. Hydrog. Energy* **2012**, *37*, 7026–7033. [[CrossRef](#)]
39. Collodi, G. Hydrogen production via steam reforming with CO<sub>2</sub> capture. *Chem. Eng. Trans.* **2010**, *19*, 37–42. [[CrossRef](#)]
40. Branco, D.A.C.; Szklo, A.S.; Schaeffer, R. CO<sub>2</sub>e emissions abatement costs of reducing natural gas flaring in Brazil by investing in offshore GTL plants producing premium diesel. *Energy* **2010**, *35*, 158–167. [[CrossRef](#)]
41. Matsumura, Y.; Nakamori, T. Steam reforming of methane over nickel catalysts at low reaction temperature. *Appl. Catal. A Gen.* **2004**, *258*, 107–114. [[CrossRef](#)]
42. Hoshi, N.; Nakamura, M.; Kida, K. Structural effects on the oxidation of formic acid on the high index planes of palladium. *Electrochem. Commun.* **2007**, *9*, 279–282. [[CrossRef](#)]
43. Ali, S.; Al-Marri, M.J.; Abdelmoneim, A.G.; Kumar, A.; Khader, M.M. Catalytic evaluation of nickel nanoparticles in methane steam reforming. *Int. J. Hydrog. Energy* **2016**, *41*, 22876–22885. [[CrossRef](#)]
44. Evans, S.E.; Staniforth, J.Z.; Darton, R.J.; Ormerod, R.M. A nickel doped perovskite catalyst for reforming methane rich biogas with minimal carbon deposition. *Green Chem.* **2014**, *16*, 4587–4594. [[CrossRef](#)]
45. Shin, G.; Yun, J.; Yu, S. Thermal design of methane steam reformer with low-temperature non-reactive heat source for high efficiency engine-hybrid stationary fuel cell system. *Int. J. Hydrog. Energy* **2017**, *42*, 14697–14707. [[CrossRef](#)]
46. Yoo, J.; Park, S.; Song, J.H.; Yoo, S.; Song, I.K. Hydrogen production by steam reforming of natural gas over butyric acid-assisted nickel/alumina catalyst. *Int. J. Hydrog. Energy* **2017**, *42*, 28377–28385. [[CrossRef](#)]
47. Wang, P.; Zhang, X.; Shi, R.; Zhao, J.; Yuan, Z.; Zhang, T. Light-Driven Hydrogen Production from Steam Methane Reforming via Bimetallic PdNi Catalysts Derived from Layered Double Hydroxide Nanosheets. *Energy Fuels* **2022**, *36*, 11627–11635. [[CrossRef](#)]
48. Andreasen, S.J.; Kær, S.K.; Sahlin, S. Control and experimental characterization of a methanol reformer for a 350 W high temperature polymer electrolyte membrane fuel cell system. *Int. J. Hydrog. Energy* **2013**, *38*, 1676–1684. [[CrossRef](#)]
49. Tojira, O.; Tepamatr, P. Catalytic Activity of Ni Based Materials Prepared by Different Methods for Hydrogen Production via the Water Gas Shift Reaction. *Catalysts* **2023**, *13*, 176. [[CrossRef](#)]
50. Men, Y.; Kolb, G.; Zapf, R.; Tiemann, D.; Wichert, M.; Hessel, V.; Loewe, H. A complete miniaturized microstructured methanol fuel processor/fuel cell system for low power applications. *Int. J. Hydrog. Energy* **2008**, *33*, 1374–1382. [[CrossRef](#)]
51. Huang, P.-H.; Kuo, J.-K.; Tu, W.-C. Investigations into the Evaporation Efficiency and Hydrogen Production Rate of Methanol-Water Fuels in a Steam Reformer Tube. *Combust. Sci. Technol.* **2019**, *192*, 1–17. [[CrossRef](#)]
52. Mei, D.; Qiu, X.; Liu, H.; Wu, Q.; Yu, S.; Xu, L.; Zuo, T.; Wang, Y. Progress on methanol reforming technologies for highly efficient hydrogen production and applications. *Int. J. Hydrog. Energy* **2022**, *47*, 35757–35777. [[CrossRef](#)]
53. Ye, R.; Xiao, S.; Lai, Q.; Wang, D.; Huang, Y.; Feng, G.; Zhang, R.; Wang, T. Advances in Enhancing the Stability of Cu-Based Catalysts for Methanol Reforming. *Catalysts* **2022**, *12*, 747. [[CrossRef](#)]
54. Fornari, A.C.; Menechini Neto, R.; Lenzi, G.G.; dos Santos, O.A.A.; de Matos Jorge, L.M. Utilization of sol-gel CuO-ZnO-Al<sub>2</sub>O<sub>3</sub> catalysts in the methanol steam reforming for hydrogen production. *Can. J. Chem. Eng.* **2017**, *95*, 2258–2271. [[CrossRef](#)]
55. Mohtashami, Y.; Taghizadeh, M. Performance of the ZrO<sub>2</sub> promoted CuZnO catalyst supported on acetic acid-treated MCM-41 in methanol steam reforming. *Int. J. Hydrog. Energy* **2019**, *44*, 5725–5738. [[CrossRef](#)]
56. Palo, D.R.; Dagle, R.A.; Holladay, J.D. Methanol steam reforming for hydrogen production. *Chem. Rev.* **2007**, *107*, 3992–4021. [[CrossRef](#)]
57. Shahsavar, H.; Taghizadeh, M.; Kiadehi, A.D. Effects of catalyst preparation route and promoters (Ce and Zr) on catalytic activity of CuZn/CNTs catalysts for hydrogen production from methanol steam reforming. *Int. J. Hydrog. Energy* **2021**, *46*, 8906–8921. [[CrossRef](#)]
58. Cheng, Z.; Zhou, W.; Lan, G.; Sun, X.; Wang, X.; Jiang, C.; Li, Y. High-performance Cu/ZnO/Al<sub>2</sub>O<sub>3</sub> catalysts for methanol steam reforming with enhanced Cu-ZnO synergy effect via magnesium assisted strategy. *J. Energy Chem.* **2021**, *63*, 550–557. [[CrossRef](#)]
59. Luo, S.; Lin, H.; Wang, Q.; Ren, X.; Hernández-Pinilla, D.; Nagao, T.; Xie, Y.; Yang, G.; Li, S.; Song, H. Triggering water and methanol activation for solar-driven H<sub>2</sub> production: Interplay of dual active sites over plasmonic ZnCu alloy. *J. Am. Chem. Soc.* **2021**, *143*, 12145–12153. [[CrossRef](#)]
60. Hou, X.; Qing, S.; Liu, Y.; Zhang, L.; Zhang, C.; Feng, G.; Wang, X.; Gao, Z.; Qin, Y. Cu<sub>1-x</sub>Mg<sub>x</sub>Al<sub>3</sub> spinel solid solution as a sustained release catalyst: One-pot green synthesis and catalytic performance in methanol steam reforming. *Fuel* **2021**, *284*, 119041. [[CrossRef](#)]
61. Chen, Y.; Li, S.; Lv, S.; Huang, Y. A novel synthetic route for MOF-derived CuO-CeO<sub>2</sub> catalyst with remarkable methanol steam reforming performance. *Catal. Commun.* **2021**, *149*, 106215. [[CrossRef](#)]

62. Wang, A.; Zhang, Y.; Fu, P.; Zheng, Q.; Fan, Q.; Wei, P.; Zheng, L. Achieving strong thermal stability in catalytic reforming of methanol over in-situ self-activated nano Cu<sub>2</sub>O/ZnO catalyst with dual-sites of Cu species. *J. Environ. Chem. Eng.* **2022**, *10*, 107676. [\[CrossRef\]](#)
63. Conant, T.; Karim, A.M.; Lebarbier, V.; Wang, Y.; Girgsdies, F.; Schlögl, R.; Datye, A. Stability of bimetallic Pd–Zn catalysts for the steam reforming of methanol. *J. Catal.* **2008**, *257*, 64–70. [\[CrossRef\]](#)
64. Shanmugam, V.; Neuberg, S.; Zapf, R.; Pennemann, H.; Kolb, G. Hydrogen production over highly active Pt based catalyst coatings by steam reforming of methanol: Effect of support and co-support. *Int. J. Hydrog. Energy* **2020**, *45*, 1658–1670. [\[CrossRef\]](#)
65. Liu, L.; Lin, Y.; Hu, Y.; Lin, Z.; Lin, S.; Du, M.; Zhang, L.; Zhang, X.-h.; Lin, J.; Zhang, Z. ZnAl<sub>2</sub>O<sub>4</sub> Spinel-Supported PdZn<sub>β</sub> Catalyst with Parts per Million Pd for Methanol Steam Reforming. *ACS Catal.* **2022**, *12*, 2714–2721. [\[CrossRef\]](#)
66. Yan, P.; Tian, P.; Cai, C.; Zhou, S.; Yu, X.; Zhao, S.; Tu, S.-T.; Deng, C.; Sun, Y. Antioxidative and stable PdZn/ZnO/Al<sub>2</sub>O<sub>3</sub> catalyst coatings concerning methanol steam reforming for fuel cell-powered vehicles. *Appl. Energy* **2020**, *268*, 115043. [\[CrossRef\]](#)
67. Ding, Y.; Zhang, T.; Ge, Z.; Li, P.; Shen, Y. High-efficiency steam reforming of methanol on the surface of a recyclable NiO/NaF catalyst for hydrogen production. *Compos. Part B Eng.* **2022**, *243*, 110113. [\[CrossRef\]](#)
68. Davda, R.R.; Shabaker, J.W.; Huber, G.W.; Cortright, R.D.; Dumesic, J.A. A review of catalytic issues and process conditions for renewable hydrogen and alkanes by aqueous-phase reforming of oxygenated hydrocarbons over supported metal catalysts. *Appl. Catal. B Environ.* **2005**, *56*, 171–186. [\[CrossRef\]](#)
69. Pipitone, G.; Zoppi, G.; Pirone, R.; Bensaid, S. A critical review on catalyst design for aqueous phase reforming. *Int. J. Hydrog. Energy* **2022**, *47*, 151–180. [\[CrossRef\]](#)
70. Pitinova, M.; Rinta-Paavola, A.; Karinen, R. Hydrogen production via aqueous-phase reforming of methanol over nickel modified Ce, Zr and La oxide supports. *Catal. Today* **2017**, *304*, 143–152. [\[CrossRef\]](#)
71. Zoppi, G.; Pipitone, G.; Gruber, H.; Weber, G.; Reichhold, A.; Pirone, R.; Bensaid, S. Aqueous phase reforming of pilot-scale Fischer-Tropsch water effluent for sustainable hydrogen production. *Catal. Today* **2020**, *367*, 239–247. [\[CrossRef\]](#)
72. Ren, X.; Wilson, M.; Gottesfeld, S. High Performance Direct Methanol Polymer Electrolyte Fuel Cell. *J. Electrochem. Soc.* **1996**, *143*, L12–L15. [\[CrossRef\]](#)
73. Zuo, Y.; Sheng, W.; Tao, W.; Li, Z. Direct methanol fuel cells system—A review of dual-role electrocatalysts for oxygen reduction and methanol oxidation. *J. Mater. Sci. Technol.* **2022**, *114*, 29–41. [\[CrossRef\]](#)
74. Alia, S.; Zhang, G.; Kisailus, D.; Li, D.; Gu, S.; Jensen, K.; Yan, Y. Porous Platinum Nanotubes for Oxygen Reduction and Methanol Oxidation Reactions. *Adv. Funct. Mater.* **2010**, *20*, 3742–3746. [\[CrossRef\]](#)
75. Sharma, C.; Awasthi, R.; Singh, R.; Sinha, A. Graphene-Manganite-Pd Hybrids as Highly Active and Stable Electrocatalysts for Methanol Oxidation and Oxygen Reduction. *Electrochim. Acta* **2014**, *136*, 166–175. [\[CrossRef\]](#)
76. Ghosh, S.; Sahu, R.; Raj, C.R. Shape-regulated high yield synthesis of electrocatalytically active branched Pt nanostructures for oxygen reduction and methanol oxidation reactions. *J. Mater. Chem.* **2011**, *21*, 11973–11980. [\[CrossRef\]](#)
77. Du, Y.; Lv, K.; Su, B.; Zhang, N.; Wang, C. Electro-reduction of oxygen and electro-oxidation of methanol at Pd monolayer-modified macroporous Pt electrode. *J. Appl. Electrochem.* **2009**, *39*, 2409–2414. [\[CrossRef\]](#)
78. Shi, Q.; Zhu, C.; Bi, C.; Xia, H.; Engelhard, M.; Du, D.; Lin, Y. Intermetallic Pd<sub>3</sub>Pb Nanowire Networks Boost Ethanol Oxidation and Oxygen Reduction Reaction with Significantly Improved Methanol Tolerance. *J. Mater. Chem. A* **2017**, *5*, 23952–23959. [\[CrossRef\]](#)
79. Uribe, J.; García-Montalvo, V.; Jiménez-Sandoval, O. A novel Rh–Ir electrocatalyst for the oxygen reduction reaction and the hydrogen and methanol oxidation reactions. *Int. J. Hydrog. Energy* **2014**, *39*, 9121–9127. [\[CrossRef\]](#)
80. Cao, J.; Du, Y.; Dong, M.; Chen, Z.; Xu, J. Template-free synthesis of chain-like PtCu nanowires and their superior performance for oxygen reduction and methanol oxidation reaction. *J. Alloy. Compd.* **2018**, *747*, 258–264. [\[CrossRef\]](#)
81. Hodnik, N.; Bele, M.; Hocevar, S. New Pt-skin electrocatalysts for oxygen reduction and methanol oxidation reactions. *Electrochem. Commun.* **2012**, *23*, 125. [\[CrossRef\]](#)
82. Wang, X.; Zhang, L.; Gong, H.; Zhu, Y.; Zhao, H.; Fu, Y. Dealloyed PtAuCu electrocatalyst to improve the activity and stability towards both oxygen reduction and methanol oxidation reactions. *Electrochim. Acta* **2016**, *212*, 277–285. [\[CrossRef\]](#)
83. Luo, I.; Zhang, R.-H.; Chen, d.; Hu, q.; Zhou, X.-W. Synthesis of 3D Thornbush-like Trimetallic CoAuPd Nanocatalysts and Electrochemical Dealloying for Methanol Oxidation and Oxygen Reduction Reaction. *ACS Appl. Energy Mater.* **2018**, *1*, 2619–2629. [\[CrossRef\]](#)
84. Yan, H.; Meng, M.; Wang, L.; Wu, A.; Tian, C.; Zhao, I.; Fu, H. Small-sized tungsten nitride anchoring into a 3D CNT-rGO framework as a superior bifunctional catalyst for the methanol oxidation and oxygen reduction reactions. *Nano Res.* **2015**, *9*, 329–343. [\[CrossRef\]](#)
85. Kulprathipanja, A.; Falconer, J. Partial oxidation of methanol for hydrogen production using ITO/Al<sub>2</sub>O<sub>3</sub> nanoparticle catalysts. *Appl. Catal. A Gen.* **2004**, *261*, 77–86. [\[CrossRef\]](#)
86. Ahmed, S.; Krumpelt, M. Hydrogen from hydrocarbon fuels for fuel cells. *Int. J. Hydrog. Energy* **2001**, *26*, 291–301. [\[CrossRef\]](#)
87. Lin, Y.-C.; Hohn, K.L.; Stagg-Williams, S.M. Hydrogen generation from methanol oxidation on supported Cu and Pt catalysts: Effects of active phases and supports. *Appl. Catal. A Gen.* **2007**, *327*, 164–172. [\[CrossRef\]](#)
88. Herdem, M.S.; Sinaki, M.Y.; Farhad, S.; Hamdullahpur, F. An overview of the methanol reforming process: Comparison of fuels, catalysts, reformers, and systems. *Int. J. Energy Res.* **2019**, *43*, 5076–5105. [\[CrossRef\]](#)

89. Chih, Y.-K.; Su, Y.-Q.; Chen, W.-H.; Lin, B.-J.; Kuo, J.-K.; You, S.; Lin, H.-P. Optimization for hydrogen production from methanol partial oxidation over Ni-Cu/Al<sub>2</sub>O<sub>3</sub> catalyst under sprays. *Int. J. Hydrog. Energy* **2022**, *47*, 40559–40572. [CrossRef]
90. Faheem, H.H.; Tanveer, H.U.; Abbas, S.Z.; Maqbool, F. Comparative study of conventional steam-methane-reforming (SMR) and auto-thermal-reforming (ATR) with their hybrid sorption enhanced (SE-SMR & SE-ATR) and environmentally benign process models for the hydrogen production. *Fuel* **2021**, *297*, 120769.
91. Richards, N.; Erickson, P. An investigation of a stratified catalyst bed for small-scale hydrogen production from methanol autothermal reforming. *Int. J. Hydrog. Energy* **2014**, *39*, 18077–18083. [CrossRef]
92. Mu, X.; Pan, L.; Liu, N.; Zhang, C.; Li, S.; Sun, G.; Wang, S. Autothermal reforming of methanol in a mini-reactor for a miniature fuel cell. *Int. J. Hydrog. Energy* **2007**, *32*, 3327–3334. [CrossRef]
93. Ghavam, S.; Vahdati, M.; Wilson, I.A.G.; Styring, P. Sustainable Ammonia Production Processes. *Front. Energy Res.* **2021**, *9*, 580808. [CrossRef]
94. Ganley, J.C.; Thomas, F.; Seebauer, E.; Masel, R.I. A priori catalytic activity correlations: The difficult case of hydrogen production from ammonia. *Catal. Lett.* **2004**, *96*, 117–122. [CrossRef]
95. Rasmussen, S.B.; Perez-Ferreras, S.; Bañares, M.A.; Bazin, P.; Daturi, M. Does pelletizing catalysts influence the efficiency number of activity measurements? Spectrochemical engineering considerations for an accurate operando study. *ACS Catal.* **2013**, *3*, 86–94. [CrossRef]
96. Cha, J.; Park, Y.; Brigljević, B.; Lee, B.; Lim, D.; Lee, T.; Jeong, H.; Kim, Y.; Sohn, H.; Mikulčić, H. An efficient process for sustainable and scalable hydrogen production from green ammonia. *Renew. Sustain. Energy Rev.* **2021**, *152*, 111562. [CrossRef]
97. Qiu, Y.; Fu, E.; Gong, F.; Xiao, R. Catalyst support effect on ammonia decomposition over Ni/MgAl<sub>2</sub>O<sub>4</sub> towards hydrogen production. *Int. J. Hydrog. Energy* **2022**, *47*, 5044–5052. [CrossRef]
98. El-Shafie, M.; Kambara, S.; Hayakawa, Y. Development of zeolite-based catalyst for enhancement hydrogen production from ammonia decomposition. *Catal. Today* **2022**, *397*, 103–112. [CrossRef]
99. Guo, J.; Chen, P. Interplay of Alkali, Transition Metals, Nitrogen, and Hydrogen in Ammonia Synthesis and Decomposition Reactions. *Acc. Chem. Res.* **2021**, *54*, 2434–2444. [CrossRef]
100. Guo, J.; Chen, Z.; Wu, A.; Fei, C.; Peikun, W.; Hu, D.; Wu, G.; Xiong, Z.; Yu, P.; Chen, P. Electronic promoter or reacting species? The role of LiNH<sub>2</sub> on Ru in catalyzing NH<sub>3</sub> decomposition. *Chem. Commun.* **2015**, *51*, 15161–15164. [CrossRef] [PubMed]
101. Guo, J.; Fei, C.; Peikun, W.; Hu, D.; Yu, P.; Wu, G.; Xiong, Z.; Chen, P. Highly Active MnN-Li<sub>2</sub>NH Composite Catalyst for Producing CO<sub>x</sub>-Free Hydrogen. *ACS Catal.* **2015**, *5*, 2708–2713. [CrossRef]
102. Coffey, R. The decomposition of formic acid catalysed by soluble metal complexes. *Chem. Commun.* **1967**, *18*, 923–924. [CrossRef]
103. Puddephatt, R.; Yap, G.A. An efficient binuclear catalyst for decomposition of formic acid. *Chem. Commun.* **1998**, *21*, 2365–2366.
104. Gao, Y.; Kuncheria, J.K.; Jenkins, H.A.; Puddephatt, R.J.; Yap, G.P. The interconversion of formic acid and hydrogen/carbon dioxide using a binuclear ruthenium complex catalyst. *J. Chem. Soc. Dalton Trans.* **2000**, *18*, 3212–3217. [CrossRef]
105. Mellmann, D.; Sponholz, P.; Junge, H.; Beller, M. Formic acid as a hydrogen storage material—Development of homogeneous catalysts for selective hydrogen release. *Chem. Soc. Rev.* **2016**, *45*, 3954–3988. [CrossRef]
106. Sordakis, K.; Dalebrook, A.F.; Laurency, G. A viable hydrogen storage and release system based on cesium formate and bicarbonate salts: Mechanistic insights into the hydrogen release step. *ChemCatChem* **2015**, *7*, 2332–2339. [CrossRef]
107. Sponholz, P.; Mellmann, D.; Junge, H.; Beller, M. Towards a practical setup for hydrogen production from formic acid. *ChemSusChem* **2013**, *6*, 1172–1176. [CrossRef]
108. Hull, J.F.; Himeda, Y.; Wang, W.-H.; Hashiguchi, B.; Periana, R.; Szalda, D.J.; Muckerman, J.T.; Fujita, E. Reversible hydrogen storage using CO<sub>2</sub> and a proton-switchable iridium catalyst in aqueous media under mild temperatures and pressures. *Nat. Chem.* **2012**, *4*, 383–388. [CrossRef]
109. Wang, W.H.; Hull, J.F.; Muckerman, J.T.; Fujita, E.; Hirose, T.; Himeda, Y. Highly efficient D<sub>2</sub> generation by dehydrogenation of formic acid in D<sub>2</sub>O through H<sup>+</sup>/D<sup>+</sup> exchange on an iridium catalyst: Application to the synthesis of deuterated compounds by transfer deuteration. *Chem. A Eur. J.* **2012**, *18*, 9397–9404. [CrossRef]
110. Lentz, N.; Albrecht, M. A Low-Coordinate Iridium Complex with a Donor-Flexible O, N-Ligand for Highly Efficient Formic Acid Dehydrogenation. *ACS Catal.* **2022**, *12*, 12627–12631. [CrossRef]
111. Li, R.; Kodaira, T.; Kawanami, H. In situ formic acid dehydrogenation observation using a UV-vis-diffuse-reflectance spectroscopy system. *Chem. Commun.* **2022**, *58*, 11079–11082. [CrossRef] [PubMed]
112. Fellay, C.; Yan, N.; Dyson, P.; Laurency, G. Selective Formic Acid Decomposition for High-Pressure Hydrogen Generation: A Mechanistic Study. *Chem. Eur. J.* **2009**, *15*, 3752–3760. [CrossRef] [PubMed]
113. Iguchi, M.; Himeda, Y.; Manaka, Y.; Matsuoka, K.; Kawanami, H. Simple Continuous High-Pressure Hydrogen Production and Separation System from Formic Acid under Mild Temperatures. *ChemCatChem* **2015**, *8*, 886–889. [CrossRef]
114. Kawanami, H.; Himeda, Y.; Laurency, G. Formic Acid as a Hydrogen Carrier for Fuel Cells Toward a Sustainable Energy System. In *Advances in Inorganic Chemistry*; Academic Press: Cambridge, MA, USA, 2017. [CrossRef]
115. Iguchi, M.; Guan, C.; Huang, K.-W.; Kawanami, H. Solvent effects on high-pressure hydrogen gas generation by dehydrogenation of formic acid using ruthenium complexes. *Int. J. Hydrog. Energy* **2019**, *44*, 28507–28513. [CrossRef]
116. Kawanami, H.; Iguchi, M.; Himeda, Y. Ligand Design for Catalytic Dehydrogenation of Formic Acid to Produce High-pressure Hydrogen Gas under Base-free Conditions. *Inorg. Chem.* **2020**, *59*, 4191–4199. [CrossRef]

117. Boddien, A.; Gärtner, F.; Jackstell, R.; Junge, H.; Spannenberg, A.; Baumann, W.; Ludwig, R.; Beller, M. Ortho-metalation of iron (0) tribenzylphosphine complexes: Homogeneous catalysts for the generation of hydrogen from formic acid. *Angew. Chem. Int. Ed.* **2010**, *49*, 8993–8996. [[CrossRef](#)]
118. Enthaler, S.; Brück, A.; Kammer, A.; Junge, H.; Irran, E.; Güllak, S. Exploring the reactivity of nickel pincer complexes in the decomposition of formic acid to CO<sub>2</sub>/H<sub>2</sub> and the hydrogenation of NaHCO<sub>3</sub> to HCOONa. *ChemCatChem* **2015**, *7*, 65–69. [[CrossRef](#)]
119. Neary, M.; Parkin, G. Nickel-catalyzed release of H<sub>2</sub> from formic acid and a new method for the synthesis of zerovalent Ni(PMe<sub>3</sub>)<sub>4</sub>. *Dalton Trans.* **2016**, *45*, 14645–14650. [[CrossRef](#)]
120. Boddien, A.; Loges, B.; Gärtner, F.; Torborg, C.; Fumino, K.; Junge, H.; Ludwig, R.; Beller, M. Iron-catalyzed hydrogen production from formic acid. *J. Am. Chem. Soc.* **2010**, *132*, 8924–8934. [[CrossRef](#)]
121. Nakajima, T.; Kamiryo, Y.; Kishimoto, M.; Imai, K.; Nakamae, K.; Ura, Y.; Tanase, T. Synergistic Cu<sub>2</sub> catalysts for formic acid dehydrogenation. *J. Am. Chem. Soc.* **2019**, *141*, 8732–8736. [[CrossRef](#)] [[PubMed](#)]
122. Wei, D.; Sang, R.; Sponholz, P.; Junge, H.; Beller, M. Reversible hydrogenation of carbon dioxide to formic acid using a Mn-pincer complex in the presence of lysine. *Nat. Energy* **2022**, *7*, 438–447. [[CrossRef](#)]
123. Huang, Y.; Wang, B.; Hangkong, Y.; Sun, Y.; Yang, D.; Cui, X.; Shi, F. Catalytic Dehydrogenation of Ethanol by Heterogeneous Catalysts. *Catal. Sci. Technol.* **2021**, *11*, 1652–1664. [[CrossRef](#)]
124. Gambo, Y.; Adamu, S.; Abdulrasheed, A.A.; Lucky, R.A.; Ba-Shammakh, M.S.; Hossain, M.M. Catalyst design and tuning for oxidative dehydrogenation of propane—A review. *Appl. Catal. A Gen.* **2021**, *609*, 117914. [[CrossRef](#)]
125. Yaacoub, L.; Dutta, I.; Werghi, B.; Chen, B.W.J.; Zhang, J.; Hamad, E.A.; Ling Ang, E.P.; Pump, E.; Sedjerari, A.B.; Huang, K.-W.; et al. Formic Acid Dehydrogenation via an Active Ruthenium Pincer Catalyst Immobilized on Tetra-Coordinated Aluminum Hydride Species Supported on Fibrous Silica Nanospheres. *ACS Catal.* **2022**, *12*, 14408–14417. [[CrossRef](#)]
126. Yu, Z.; Yang, Y.; Yang, S.; Zheng, J.; Hao, X.; Wei, G.; Bai, H.; Abudula, A.; Guan, G. Selective dehydrogenation of aqueous formic acid over multifunctional  $\gamma$ -Mo<sub>2</sub>N catalysts at a temperature lower than 100 °C. *Appl. Catal. B Environ.* **2022**, *313*, 121445. [[CrossRef](#)]
127. Ding, Y.; Peng, W.; Zhang, L.; Xia, J.; Feng, G.; Lu, Z.-H. Chromic hydroxide-decorated palladium nanoparticles confined by amine-functionalized mesoporous silica for rapid dehydrogenation of formic acid. *J. Colloid Interface Sci.* **2023**, *630*, 879–887. [[CrossRef](#)]
128. Sun, X.; Zhang, G.; Yao, Q.; Li, H.; Feng, G.; Lu, Z.-H. Amine-Functionalized Carbon Bowl-Supported Pd-La(OH)<sub>3</sub> for Formic Acid Dehydrogenation. *Inorg. Chem.* **2022**, *61*, 18102–18111. [[CrossRef](#)] [[PubMed](#)]
129. Wang, Z.-L.; Yan, J.-M.; Ping, Y.; Wang, H.-L.; Zheng, W.-T.; Jiang, Q. An Efficient CoAuPd/C Catalyst for Hydrogen Generation from Formic Acid at Room Temperature. *Angew. Chem.* **2013**, *125*, 4502–4505. [[CrossRef](#)]
130. Liu, D.-X.; Zhou, Y.-T.; Zhu, Y.-F.; Chen, Z.-Y.; Yan, J.-M.; Jiang, Q. Tri-metallic AuPdIr nanoalloy towards efficient hydrogen generation from formic acid. *Appl. Catal. B Environ.* **2022**, *309*, 121228. [[CrossRef](#)]
131. Kumar, G.; Banu, R.; Xia, A.; Sivagurunathan, P.; Saratale, G. A critical review on anaerobic digestion of microalgae and macroalgae and co-digestion of biomass for enhanced methane generation. *Bioresour. Technol.* **2018**, *262*, 319–332. [[CrossRef](#)]
132. Ayodele, B.; bin Tuan Abdullah, T.A.R.; Ali Alsaffar, M.; Mustapa, S.; Salleh, S. Recent advances in renewable hydrogen production by thermo-catalytic conversion of biomass-derived glycerol: Overview of prospects and challenges. *Int. J. Hydrog. Energy* **2019**, *45*, 18160–18185. [[CrossRef](#)]
133. Gautam, P.; Neha; Upadhyay, S.; Dubey, S. Bio-methanol as a renewable fuel from waste biomass: Current trends and future perspective. *Fuel* **2020**, *273*, 117783. [[CrossRef](#)]
134. Manocchio, C.; Andrade, B.R.; Rodriguez, R.; Moraes, B. Ethanol from biomass: A comparative overview. *Renew. Sustain. Energy Rev.* **2017**, *80*, 743–755. [[CrossRef](#)]
135. Pal, D.B.; Singh, A.; Bhatnagar, A. A review on biomass based hydrogen production technologies. *Int. J. Hydrog. Energy* **2022**, *47*, 1461–1480. [[CrossRef](#)]
136. Dincer, I.; Acar, C. Review and Evaluation of Hydrogen Production Methods for Better Sustainability. *Altern. Energy Ecol. (ISJAEE)* **2016**, *11*, 14–36. [[CrossRef](#)]
137. Zhao, L.; Wu, K.-K.; Chen, C.; Ren, H.-Y.; Wang, Z.-H.; Nan, J.; Yang, S.; Cao, G.; Ren, N.-Q. Role of residue cornstalk derived biochar for the enhanced bio-hydrogen production via simultaneous saccharification and fermentation of cornstalk. *Bioresour. Technol.* **2021**, *330*, 125006. [[CrossRef](#)]
138. Fahmy, T.; Fahmy, Y.; Mobarak, F.; El-Sakhawy, M.; Abouzeid, R. Biomass pyrolysis: Past, present, and future. *Environ. Dev. Sustain.* **2020**, *22*, 17–32. [[CrossRef](#)]
139. Pokorna, E.; Postelmans, N.; Jenicek, P.; Schreurs, S.; Carleer, R.; Yperman, J. Study of bio-oils and solids from flash pyrolysis of sewage sludges. *Fuel* **2009**, *88*, 1344–1350. [[CrossRef](#)]
140. Valle, B.; Aramburu, B.; Benito, P.; Bilbao, J.; Gayubo, A. Biomass to hydrogen-rich gas via steam reforming of raw bio-oil over Ni/La<sub>2</sub>O<sub>3</sub>- $\alpha$ Al<sub>2</sub>O<sub>3</sub> catalyst: Effect of space-time and steam-to-carbon ratio. *Fuel* **2018**, *216*, 445–455. [[CrossRef](#)]
141. Demirbas, M. Hydrogen from Various Biomass Species via Pyrolysis and Steam Gasification Processes. *Energy Sources* **2006**, *28*, 245–252. [[CrossRef](#)]
142. Florin, N.; Harris, A. Enhanced hydrogen production from biomass with in situ carbon dioxide capture using calcium oxide sorbents. *Chem. Eng. Sci.* **2008**, *63*, 287–316. [[CrossRef](#)]

143. Manoharan, Y.; Hosseini, S.E.; Butler, B.; Alzahrani, H.; Senior, B.T.F.; Ashuri, T.; Krohn, J. Hydrogen fuel cell vehicles; current status and future prospect. *Appl. Sci.* **2019**, *9*, 2296. [[CrossRef](#)]
144. Youon Technology Co., Ltd. Available online: <https://www.youonbikeshare.com/> (accessed on 22 February 2022).
145. Wróbel, K.; Wróbel, J.; Tokarz, W.; Lach, J.; Podsadni, K.; Czerwiński, A. Hydrogen Internal Combustion Engine Vehicles: A Review. *Energies* **2022**, *15*, 8937. [[CrossRef](#)]
146. Wakayama, N.; Morimoto, K.; Kashiwagi, A.; Saito, T. Development of Hydrogen Rotary Engine Vehicle. In Proceedings of the 16th World Hydrogen Energy Conference, Lyon, France, 13–16 June 2006.
147. Liu, W.; Zuo, H.; Wang, J.; Xue, Q.; Ren, B.; Yang, F. The production and application of hydrogen in steel industry. *Int. J. Hydrog. Energy* **2021**, *46*, 10548–10569. [[CrossRef](#)]
148. DATAZERO. Available online: <https://www.irit.fr/datazero/index.php/en/> (accessed on 10 February 2023).
149. Sun.Storage Underground. Final Report. Available online: <https://www.underground-sun-storage.at/en/public-relations/-/publications/publications-1.html> (accessed on 10 February 2023).

**Disclaimer/Publisher’s Note:** The statements, opinions and data contained in all publications are solely those of the individual author(s) and contributor(s) and not of MDPI and/or the editor(s). MDPI and/or the editor(s) disclaim responsibility for any injury to people or property resulting from any ideas, methods, instructions or products referred to in the content.